Structure and ferroelectric properties of epitaxial $(1-x)BiFeO_3-xBaTiO_3$ solid solution films

2008 J. Phys.: Condens. Matter 20 415208

(http://iopscience.iop.org/0953-8984/20/41/415208)

J. Phys.: Condens. Matter **20** (2008) 415208 (6pp) doi:10.1088/0953-8984/20/41/415208

Structure and ferroelectric properties of epitaxial $(1-x)BiFeO_3$–$xBaTiO_3$ solid solution films

P Murugavel[1], J-H Lee[2], J Y Jo[2], Hye Yeong Sim[2], J-S Chung[3], Younghun Jo[4] and Myung-Hwa Jung[4]

[1] Department of Physics, Indian Institute of Technology Madras, Chennai 600 036, India
[2] ReCOE & FPRD, School of Physics and Astronomy, Seoul National University, Seoul 151-747, Korea
[3] Department of Physics and CAMDRC, Soongsil University, Seoul 156-743, Korea
[4] Quantum Material Research Team, Korea Basic Science Institute, Daejeon 305-333, Korea

E-mail: muruga@physics.iitm.ac.in

Received 11 December 2007, in final form 2 August 2008
Published 12 September 2008
Online at stacks.iop.org/JPhysCM/20/415208

Abstract

We fabricated epitaxial $(1-x)BiFeO_3$–$xBaTiO_3$ ($x = 0.1$–0.7) solid solution films on niobium doped $SrTiO_3(001)$ substrate. The x-ray diffraction analysis of the films indicates compressively strained growth for the composition $x < 0.3$ and strain relaxed growth for the composition $x \geqslant 0.3$. Correspondingly, the films showed a structural change from a rhombohedral (or modified monoclinic M_A) phase to a tetragonal phase near the composition $x \sim 0.3$. Interestingly the ferroelectric measurements showed a distinct difference between the compositions, with the boundary at $x \sim 0.3$, above which the films remain in a highly resistive state. The magnetic measurements revealed a weak ferromagnetic signature for the films of composition $x \leqslant 0.5$.

1. Introduction

In recent times, there has been a flurry of research activities on the multiferroic materials, with the possibility of controlling the ferroelectric/magnetic property by means of applied magnetic/electric field [1–6]. Among them, $BiFeO_3$ is a promising material due to its large reported ferroelectric polarization in films [5, 7]. Bulk $BiFeO_3$ single crystals exhibit a ferroelectric transition at ≈1100 K [8], and an antiferromagnetic Néel temperature at ≈643 K [9]. In the bulk, $BiFeO_3$ has a distorted perovskite structure with rhombohedral crystal symmetry (lattice parameter $a = 3.958$ Å, $\alpha = 89.30°$) [10] and the reported saturation polarization (P_s) value is only 6.1 $\mu C\ cm^{-2}$ at 77 K [11]. However, Wang *et al* [5] reported remnant polarization (P_r) values of 50–60 $\mu C\ cm^{-2}$ in $BiFeO_3$ epitaxial films. Although the enhancement was initially attributed to the tetragonal symmetry and the strain effect, the first-principles calculations predicted that $BiFeO_3$ crystal in its rhombohedral crystal symmetry could possess a theoretical *Pr* value of around 100 $\mu C\ cm^{-2}$ [12, 13].

However, the measurement of polarization in $BiFeO_3$ is hampered by large leakage current due to deviation from oxygen stoichiometry and defects. Some workers have even argued that the enhanced polarization of $BiFeO_3$ in films reported could be attributed to the extra charge inflow based on the leakage current [14]. Hence improvement of the electrical resistivity is essential for successful development of this material for practical use. Although there were a few earlier attempts to overcome the leakage current by forming solid solutions with highly insulating materials, either the polarization value is small [15] or the characterization is limited to the bulk [16, 17]. The aim of this study is to fabricate and investigate a series of solid solution films of $BiFeO_3$ and an insulating perovskite. We used $BaTiO_3$ as an insulating perovskite to form solid solutions. The fabricated $(1-x)BiFeO_3$–$xBaTiO_3$ ($x = 0.1$–0.7) films are characterized for their structure, electric and magnetic properties. Our results demonstrate a structural change from a rhombohedral (or modified monoclinic M_A) phase to a tetragonal phase with a high polarization value in the former (∼60 $\mu C\ cm^{-2}$ at 150 K) compared to the latter phase (∼24 $\mu C\ cm^{-2}$ at 300 K). We also showed that the leakage current is highly reduced in our solid solution films of composition $x > 0.3$.

2. Experimental details

We have fabricated the $(1-x)BiFeO_3$–$xBaTiO_3$ ($x = 0.1$–0.7) solid solution films on (001) oriented conducting Nb–$SrTiO_3$(001) (Nb–STO) substrates by a pulsed laser deposition technique (PLD). The targets are made from the powders of $Bi_{1.1}FeO_3$ and $BaTiO_3$ by mixing them in appropriate ratios. The mixed powders are subjected to calcinations with intermediate grindings. Final sintering of the targets is carried out at temperatures in the range of 850–950 °C. The films are deposited at 720 °C by maintaining the PLD chamber at an oxygen partial pressure of 100 mTorr. We used a KrF excimer laser (248 nm, Lambda Physik), with laser fluence and repetition rates of 1.5 J cm^{-2} and 3 Hz, respectively for all the depositions. The films are characterized by x-ray diffraction (XRD) for their structure. We used a Rigaku x-ray diffractometer for θ–2θ scanning of our films. ϕ scans and reciprocal space mapping were recorded using a Bruker X'Pert four-circle high resolution x-ray diffractometer using Cu Kα radiation ($\lambda = 0.154\,18$ nm). For electrical measurement; gold top-electrodes 100 μm in diameter are deposited using a shadow mask. The polarization versus electric field (P–E) hysteresis loops are measured using a low temperature probe station (Desert Cryogenics) and T–F analyser (aixACCT) at 2 kHz. Magnetic properties are measured using a magnetic property measurement system (Quantum Design).

3. Results and discussion

3.1. Structural properties

The films with $x = 0.1$–0.7 were grown epitaxially with their c-axes perpendicular to the plane of the substrate. As an example, in figure 1(a) we show the XRD θ–2θ pattern of the $x = 0.5$ film. In the XRD pattern, we see only the (00l) peaks along with substrate peaks. No other impurity peaks are seen in the pattern, confirming single-phase formation of the film. For clarity, in the inset of figure 1(a), we show rocking curve scans of the (001) plane for $x = 0$, 0.2 and 0.5 films. The inset shows that the full width at half-maximum values of the rocking curves are <0.1°, confirming good crystalline quality of the films. In figure 1(b), the XRD θ–2θ patterns around the (001) reflection for the films with $x = 0.1$–0.7 along with the pure $BiFeO_3$ film are shown. Interestingly, the solid solution films with initial $BaTiO_3$ concentrations of $x = 0.1$ and 0.2 display a large shift in (00l) reflections towards lower angle, indicating enlarged out-of-plane lattice parameter (c) as compared to the parent $BiFeO_3$ film. Note that the $BiFeO_3$ ($a = 3.952$ Å) is expected to form under compressive strain on Nb–STO ($a = 3.905$ Å) [5]. Since the lattice parameter of $BaTiO_3$ (4.2 Å) is larger than that of $BiFeO_3$, the enlarged c parameter of the solid solution films could be the result of clamping of the in-plane parameter (a) with the substrate lattice due to compressive strain. To confirm the epitaxy of these films, we have done off axis ϕ scans along the (102) direction for both the films and the substrate. Four distinct peaks separated by 90° (not shown in the figure) observed in both cases clearly indicate fourfold symmetry with in-plane coherence of these heterostructures. All the films on

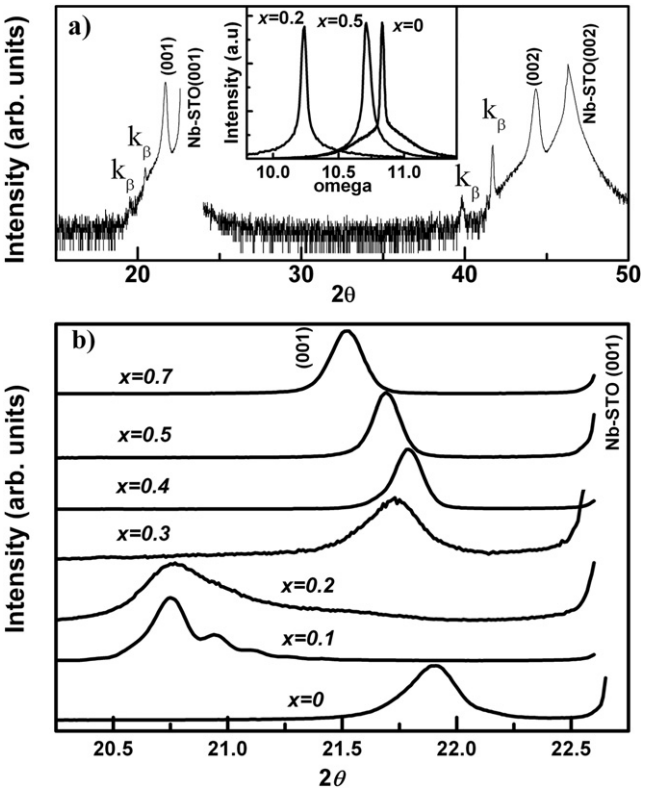

Figure 1. (a) θ–2θ XRD scan of $0.5BiFeO_3$–$0.5BaTiO_3$ solid solution film on Nb–STO substrate. The inset shows the rocking curve for (001) film peaks for the compositions $x = 0$, 0.2 and 0.5. (b) θ–2θ XRD scans around Nb–STO(001) peaks for the compositions $x = 0$, 0.1, 0.2, 0.3, 0.4, 0.5, and 0.7.

Nb–STO(001) substrate have in-plane [100] ∥ [100] epitaxial relationships. However, large changes in the c lattice parameter near the composition $x = 0.3$ suggest a possible structural transition.

To get further insight, we obtained x-ray reciprocal space maps (RSMs) around the asymmetric (103) reflection. Figures 2(a), (b), (c), (d), (e), and (f) show the RSMs of $x = 0$, 0.1, 0.2, 0.3, 0.4, and 0.5 films on Nb–STO substrate, respectively, in reciprocal lattice units (rlu). These RSMs show clear (103) reflections of the film and the Nb–STO substrate in the $H\,0\,L$ scattering plane. Note that film and substrate peaks in figures 2(a), (b) and (c) are on the same H-value line (indicated by the dotted line), indicating that the $x = 0$ and 0.1 films are grown coherently on Nb–STO substrate. However, the peaks of $x = 0.3$, 0.4 and 0.5 films shown in figures 2(d), (e), and (f), respectively, are deviated from the substrate peak, indicating the strain relaxed growth. Also both $x = 0$ and 0.1 films are grown under compressive strained conditions with the same in-plane lattice as the substrate. This is further inferred from figure 3 where the lattice parameters calculated from the mapping data are plotted. The $BiFeO_3$ film with in-plane and out-of-plane lattice parameters of 3.905 Å and 4.043 Å, respectively differs greatly from the rhombohedral bulk lattice (3.96 Å). Upon doping, the $BiFeO_3$ shows 6% increase in the out-of-plane lattice parameter with 10% $BaTiO_3$. However, the in-plane lattice parameter a is nearly matched with the

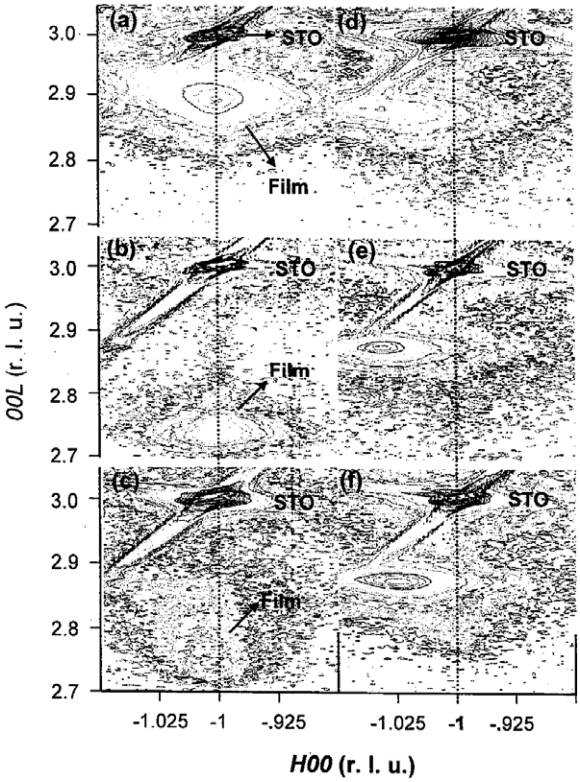

Figure 2. X-ray reciprocal space mapping around the asymmetric (103) reflections of $(1-x)BiFeO_3$–$xBaTiO_3$ solid solution films: (a) $x = 0$, (b) $x = 0.1$, (c) $x = 0.2$, (d) $x = 0.3$, (e) $x = 0.4$, and (f) $x = 0.5$.

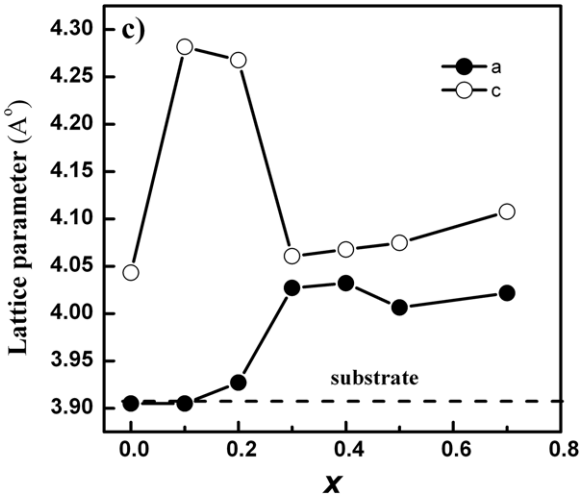

Figure 3. In-plane and out-of-plane lattice parameter variation with respect to the $BaTiO_3$ composition.

substrate lattice (indicated by the dotted line in figure 3). In solid solution films the A-site Bi^{3+} will be replaced by Ba^{2+} and the B-site Fe^{3+} will be replaced by Ti^{4+}. The ionic radii of Bi^{3+}, Fe^{3+}, Ba^{2+} and Ti^{4+} are 1.03 Å, 0.64 Å, 1.42 Å and 0.605 Å, respectively. So the substitution of the smaller ion Bi^{3+} by larger ion Ba^{2+} will increase the overall volume of the unit cell. As a result the $(1-x)BiFeO_3$–$xBaTiO_3$ films should show increase in volume with x. Hence the enhancement in the c lattice parameter of our $x = 0.1$ film is a manifestation of increase in volume and clamping of the in-plane lattice with the substrate. With increase in doping, at $x = 0.2$, figure 2(c) shows that the film starts relaxing. The calculated volume of the solid solution film did not show systematic increase with increase in x. One reason could be the following. Although A-site substitution by Ba^{2+} will increase the unit cell volume, this is reversed for the Ti^{4+} substitution on site B. So the doping of $BaTiO_3$ should be responsible for the fluctuation of the unit cell volume. However, other possible reasons could not be overlooked.

Upon further increase in x above 0.3, the films are relaxed from the substrate induced strain and the lattice parameters show nearly linear variation with the concentration x. Note that in the bulk the parent $BiFeO_3$ and $BaTiO_3$ exist in rhombohedral and tetragonal perovskite structure, respectively. Although epitaxial $BiFeO_3$ film is reported to form in tetragonal structure [5], recent synchrotron x-ray diffraction studies reveal that it could be in the rhombohedral (or modified monoclinic M_A) phase instead of the tetragonal one [18]. Also, the bulk $(1-x)BiFeO_3$–$xBaTiO_3$ solid solution undergoes a phase transition from rhombohedral to cubic structure near the composition $x \sim 0.4$ [16, 17]. So the change in lattice parameters of our films near the composition $x \sim 0.3$ could be attributed to a structural transition from a rhombohedral to a tetragonal phase.

To verify this further we have obtained reciprocal space maps of the films around the (113) reflection at different azimuthal angles (ϕ). Figures 4(a) and (b) show reciprocal space maps of the films with $x = 0.1$ and $x = 0.2$ at $\phi = 45°$ and $\phi = 225°$, respectively. The RSM of the film with $x = 0.2$ shows peak splitting due to the existence of two domains. Also upon 180° azimuthal rotation, the RSM of the film with $x = 0.2$ reveals a change in peak splitting along the $[00L]$ direction, indicating planes with different d spacings [19], whereas the $x = 0.3$ film shows no such peak splitting. These findings confirm that the crystal structure of the $x = 0.2$ film is rhombohedral (or modified monoclinic M_A) while that of the $x = 0.3$ film is tetragonal. Hence the HRXRD RSM confirm that the $(1-x)BiFeO_3$–$xBaTiO_3$ solid solution films undergo a structural transition from a modified monoclinic M_A phase to a tetragonal phase with a phase boundary at $x = 0.3$.

3.2. Leakage current

For the leakage current, we measured the current versus electric field for all the compositions, and the resultant curves for the $x = 0.1$, 0.2, 0.4 and 0.5 films at 300 K are shown in figure 5. At room temperature, the films with $x = 0.1$ and 0.2 show high leakage current, indicating their low resistive state. On the other hand, with increase in $BaTiO_3$ concentration, i.e. when $x \geqslant 0.3$, the films show a leakage current nearly three orders of magnitude lower as compared to the films with $x = 0.1$–0.2. With this improvement of electrical resistivity, the films of composition $x > 0.3$ are expected to show polarization at room temperature.

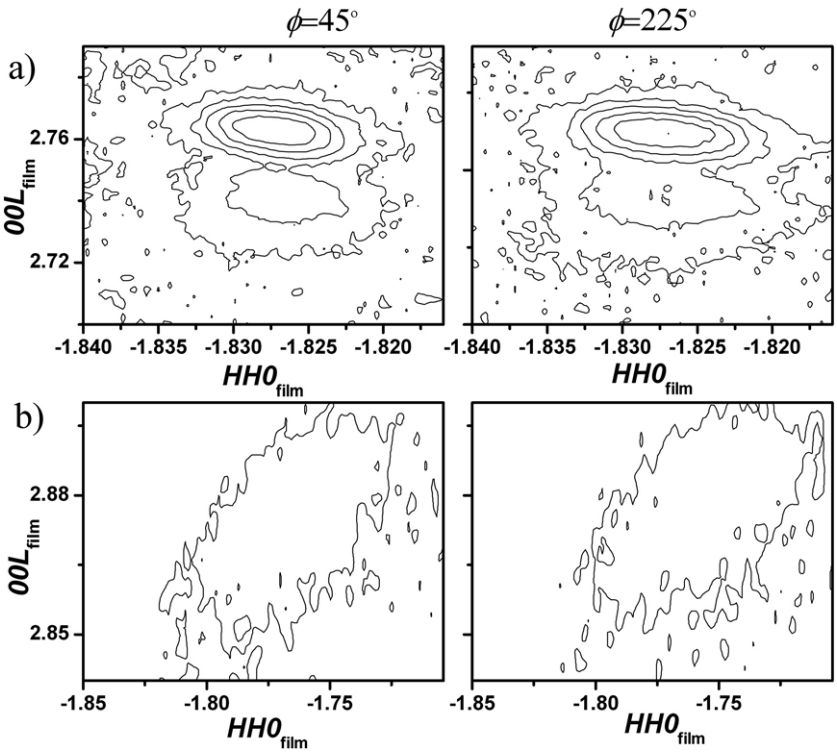

Figure 4. X-ray reciprocal space mapping around (113) reflections of $(1-x)BiFeO_3$–$xBaTiO_3$ solid solution films: (a) $x = 0$ and (b) $x = 0.3$ at $\phi = 45°$ and 225°.

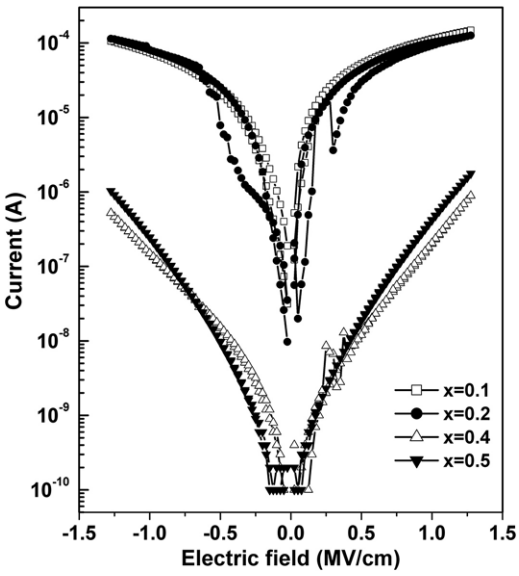

Figure 5. Leakage current versus electric field curves for the solid solution films.

3.3. Ferroelectric properties

Although the high leakage current in some of our samples could prevent polarization measurement at room temperature, their magnitude could be minimized at low temperatures. Hence to investigate the ferroelectric properties, we carried out P–E measurement from 70 to 300 K and the results are shown in figure 6 at selected temperatures. As expected, we were able to measure the P–E hysteresis loops for the films with $x = 0.1$ and 0.2 up to the temperatures 125 and 150 K, respectively and the respective graphs are shown in figures 6(a) and (b). The graphs indicate that the films do indeed show ferroelectric properties with high polarization value. For example, the films with $x = 0.2$ exhibit good P–E loops with a maximum Pr value of ∼60 μC cm^{-2} and the coercive field of 0.7 MV cm^{-1}. These are comparable to the reported room temperature values for $BiFeO_3$ films [5]. However, at higher $BaTiO_3$ composition, x, we were successfully able to measure the P–E loops at 300 K and the results for the compositions $x = 0.3$, 0.4, 0.5 and 0.7 are shown in figures 6(c)–(f), respectively. From figure 6, the Pr values for the films with $x = 0.4$, 0.5, and 0.7 were calculated to be 14, 24 and 12 μC cm^{-2} at 1.5 MV cm^{-1} applied field, respectively. Note that the high polarization values are obtained only for films which are in the rhombohedral phase, and the films grown in the tetragonal phase display reduced polarization. However, the polarization values are higher than the value of 2.5 μC cm^{-2} reported for epitaxial solid solution film [15]. Our results show that the leakage currents are reduced in the solid solution films and the films are showing reasonable polarization values compared to the parent $BiFeO_3$ film [5].

3.4. Magnetic properties

The magnetic measurements reveal weak ferromagnetic signatures at 300 K for all the films except the one at the composition $x = 0.7$, which shows a paramagnetic signature. Figure 7 shows the magnetization versus magnetic field

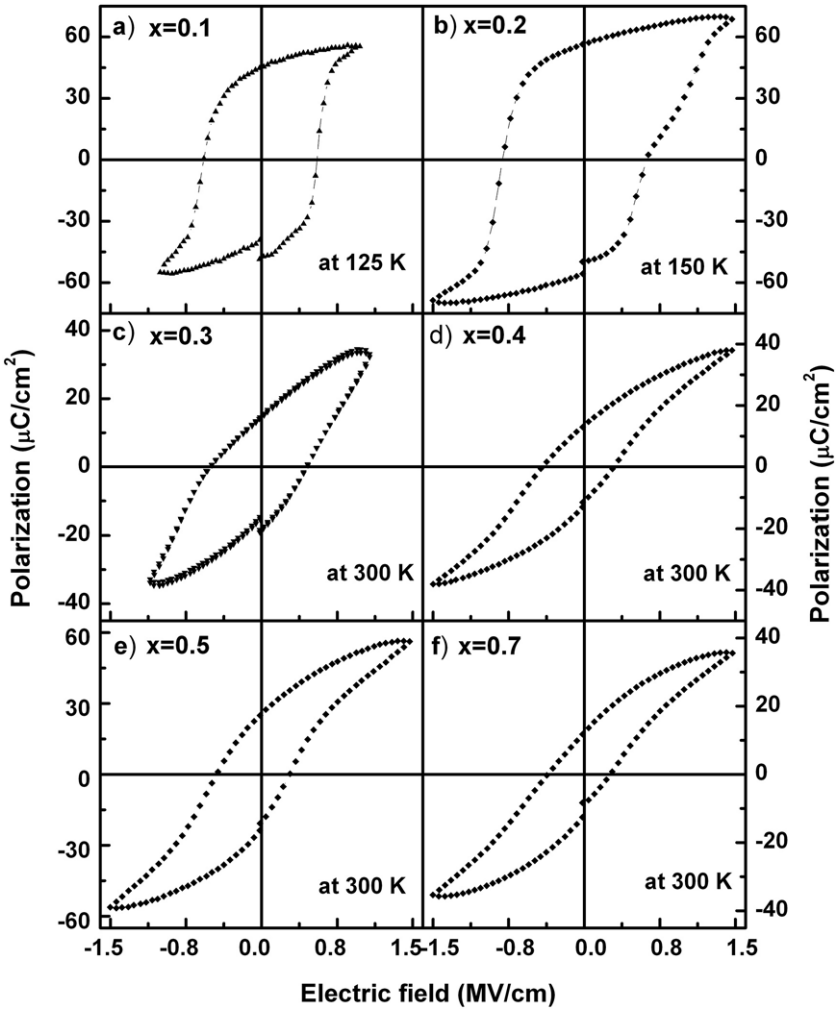

Figure 6. Polarization versus electric field hysteresis curves of the films: (a) $x = 0.1$ at 125 K, (b) $x = 0.2$ at 150 K, (c) $x = 0.3$ at 300 K, (d) $x = 0.4$ at 300 K, (e) $x = 0.5$ at 300 K, and (f) $x = 0.7$ at 300 K.

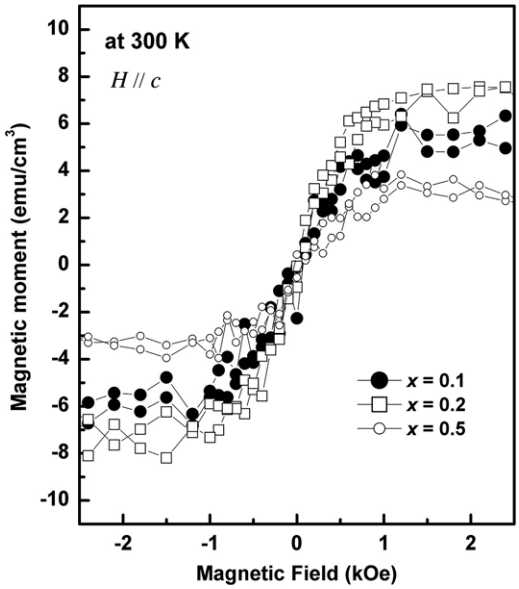

Figure 7. Magnetization versus magnetic field for the films with $x = 0$, 0.2 and 0.3 composition measured at 300 K by applying the field along the out-of-plane direction.

(M–H) curves measured by applying the field parallel to the c-axis. The weak magnetic signal makes the data look noisy. For clarity, we show the M–H curves of the samples with $x = 0.1$, 0.2 and 0.5. Although the samples are not showing complete saturation, the magnetization value of the film with $x = 0.1$ at 0.25 T is around 0.05 μ_B per unit cell ($\sim$8 emu cm^{-3}). This is of the same order of magnitude as the bulk [20] and the density functional calculations for an unstrained film [12] of $BiFeO_3$. However, the films show an initial decrease followed by an increase in magnetization with x. The increase in magnetization above $x = 0.2$ could be due to the bulk magnetization originating from the statistical distribution of Fe^{3+} and Ti^{4+} ions in the perovskite octahedra [21]. However, the unsaturated M–H curve even at high applied magnetic field (not shown in the figure) indicates the basic antiferromagnetic nature of the samples.

4. Conclusions

In conclusion, we have deposited epitaxial $(1 - x)BiFeO_3$–$xBaTiO_3$ solid solution films on Nb–$SrTiO_3$ substrates by a

pulsed laser deposition technique. The x-ray diffraction analysis shows a structural phase transition from a rhombohedral (or modified monoclinic) phase to a tetragonal phase near the composition $x = 0.3$. In the rhombohedral phase the films exhibit the polarization value of $\sim$60 μC cm^{-2} at 150 K with leakage currents dominating as we increase the temperature. However, the ferroelectric measurement on $(1 - x)BiFeO_3$–$xBaTiO_3$ films demonstrates that the leakage current could be reduced above the composition $x = 0.3$. Also, these films display reasonable polarization values with maximum remnant polarization of 24 μC cm^{-2} at 300 K for $x = 0.5$, indicating its possibility for suitable practical applications. Although the films exhibit weak ferromagnetic signatures, further investigations are still needed in order to understand its magnetic ordering. It would be interesting to see magnetoelectric measurements on these solid solution films.

Acknowledgment

The authors thank Professor T W Noh of Seoul National University, Seoul, for his encouragement, suggestions and support.

References

[1] Kimura T, Goto T, Shintani H, Ishizaka K, Arima T and Tokura Y 2003 *Nature* **426** 55
[2] Hur N, Park S, Sharma P A, Ahn J S, Guha S and Cheong S W 2004 *Nature* **429** 392
[3] Lottermoser T, Lonkai T, Amann U, Hohlwein D, Ihringer J and Fiebig M 2004 *Nature* **430** 541
[4] Fiebig M, Lottermoser T, Frölich D, Goltsev A V and Pisarev A V 2002 *Nature* **419** 818
[5] Wang J, Neaton J B, Zheng H, Nagarajan V, Ogale S B, Liu B, Viehland D, Vaithyanathan V, Schlom D G, Waghmare U V, Spaldin N A, Rabe K M, Wuttig M and Ramesh R 2003 *Science* **299** 1719
[6] Prellier W, Singh M P and Murugavel P 2005 *J. Phys.: Condens. Matter* **17** R803
[7] Zhao T, Scholl A, Zavaliche F, Lee K, Barry M, Doran A, Cruz M P, Chu Y H, Ederer C, Spaldin N A, Das R R, Kim D M, Baek S H, Eom C B and Ramesh R 2006 *Nat. Mater.* **5** 823
[8] Smolenskii G A, Isupov V, Agranovskaya A and Krainik N 1961 *Sov. Phys.—Solid State* **2** 2651
[9] Smolenskii G A, Yudin V, Sher E and Stolypin Y E 1963 *Sov. Phys.—JETP* **16** 622
[10] Bucci J D, Robertson B K and James W J 1972 *J. Appl. Crystallogr.* **5** 187
[11] Teague J R, Gerson R and James W J 1970 *Solid State Commun.* **8** 1073
[12] C Ederer J R and Spaldin N A 2005 *Phys. Rev.* B **71** 060401
[13] Neaton J B, Ederer C, Waghmare U V, Spaldin N A and Rabe K M 2005 *Phys. Rev.* B **71** 014113
[14] Eerenstein W, Morrison F D, Dho J, Blamire M G, Scott J F and Mathur N D 2005 *Science* **307** 1203
[15] Ueda K, Tabata H and Kawai T 1999 *Appl. Phys. Lett.* **75** 555
[16] Mahesh Kumar M, Srinath S, Kumar G S and Suryanarayana S V 1998 *J. Magn. Magn. Mater.* **188** 203
[17] Kim J S, Cheon C I, Lee C H and Jang P W 2004 *J. Appl. Phys.* **96** 468
[18] Xu G, Hiraka H, Shirane G, Li J, Wang J and Viehland D 2005 *Appl. Phys. Lett.* **86** 182905
[19] Li J F, Wang J, Wuttig M, Ramesh R, Wang N, Ruette B, Pyatakov P, Zvezdin A K and Viehland D 2004 *Appl. Phys. Lett.* **84** 5261
[20] Smolenskii G A, Yudin V M, Sher E S and Stolypin Y E 1963 *Sov. Phys.—JETP* **16** 622
[21] Gehring G A 1994 *Ferroelectrics* **161** 275